Hindawi Publishing Corporation
Journal of Nanomaterials
Volume 2016, Article ID 1039258, 11 pages
http://dx.doi.org/10.1155/2016/1039258

*Research Article*

# $^{177}$Lu-Dendrimer Conjugated to Folate and Bombesin with Gold Nanoparticles in the Dendritic Cavity: A Potential Theranostic Radiopharmaceutical

**Héctor Mendoza-Nava,[1,2] Guillermina Ferro-Flores,[1] Flor de María Ramírez,[1] Blanca Ocampo-García,[1] Clara Santos-Cuevas,[1] Liliana Aranda-Lara,[1,2] Erika Azorín-Vega,[1] Enrique Morales-Avila,[2] and Keila Isaac-Olivé[2]**

[1]*Instituto Nacional de Investigaciones Nucleares (ININ), 52750 Ocoyoacac, MEX, Mexico*
[2]*Universidad Autónoma del Estado de México, 50180 Toluca, MEX, Mexico*

Correspondence should be addressed to Guillermina Ferro-Flores; ferro_flores@yahoo.com.mx

Received 15 April 2016; Revised 28 June 2016; Accepted 29 June 2016

Academic Editor: Piersandro Pallavicini



$^{177}$Lu-labeled nanoparticles conjugated to biomolecules have been proposed as a new class of theranostic radiopharmaceuticals. The aim of this research was to synthesize $^{177}$Lu-dendrimer(PAMAM-G4)-folate-bombesin with gold nanoparticles (AuNPs) in the dendritic cavity and to evaluate the radiopharmaceutical potential for targeted radiotherapy and the simultaneous detection of folate receptors (FRs) and gastrin-releasing peptide receptors (GRPRs) overexpressed in breast cancer cells. p-SCN-Benzyl-DOTA was conjugated in aqueous-basic medium to the dendrimer. The carboxylate groups of Lys$^1$Lys$^3$(DOTA)-bombesin and folic acid were activated with HATU and also conjugated to the dendrimer. The conjugate was mixed with 1% $HAuCl_4$ followed by the addition of $NaBH_4$ and purified by ultrafiltration. Elemental analysis (EDS), particle size distribution (DLS), TEM analysis, UV-Vis, and infrared and fluorescence spectroscopies were performed. The conjugate was radiolabeled using $^{177}LuCl_3$ or $^{68}GaCl_3$ and analyzed by radio-HPLC. Studies confirmed the dendrimer functionalization with high radiochemical purity (>95%). Fluorescence results demonstrated that the presence of AuNPs in the dendritic cavity confers useful photophysical properties to the radiopharmaceutical for optical imaging. Preliminary binding studies in T47D breast cancer cells showed a specific cell uptake (41.15 ± 2.72%). $^{177}$Lu-dendrimer(AuNP)-folate-bombesin may be useful as an optical and nuclear imaging agent for breast tumors overexpressing GRPR and FRs, as well as for targeted radiotherapy.

## 1. Introduction

Dendrimers are hyperbranched polymeric structures varying in their initiator core, repeating units, terminal functionality, charge, and solubility profile. A drug can be entrapped either within the internal cavities or conjugated to peripheral functional groups of the dendrimer. Polyamidoamine (PAMAM) dendrimers are spherical macromolecules composed of repeating polyamidoamine units which are known to have low biological toxicity, good biocompatibility, and in vivo stability [1, 2].

Gold nanoparticles (AuNPs) conjugated to peptides or biomolecules with target-specific recognition produce stable multimeric systems with target-specific molecular recognition. Plasmonic AuNPs can be fluorescent when they are prepared by thermal reduction procedures or when they are designed to absorb in the near infrared region; therefore, AuNPs can also function as optical imaging agents [3, 4].

Over the last two decades, several experimental evidences have suggested that the gastrin-releasing peptide (GRP) and other bombesin-like peptides act as growth factors in many types of cancer [5]. Overexpression of gastrin-releasing peptide receptors (GRPR) is present in 96% of breast cancer tissues [6]. Different bombesin analogues with high affinity for GRPR have been evaluated in preclinical studies for receptor-specific imaging and therapy [5]. Clinical studies

in women using radio-bombesin derivatives have shown successful radionuclide imaging of breast tumors [7–10]. In particular, the GRPR is highly expressed in T47D human breast cells, and that is the reason why these cells have been used as tumor models to evaluate new bombesin probes [6, 11–13].

Folate receptor-$\alpha$ (FR$\alpha$) is a membrane-bound protein with high affinity for binding and transporting folate into cells. Folate is a basic component of cell metabolism and DNA synthesis and repair. Cancer cells, which rapidly divide, have an increased requirement for folate to maintain DNA synthesis, an observation supported by the widespread use of antifolates in cancer chemotherapy [14, 15].

The overexpression of FR$\alpha$ protein has been confirmed in all clinical breast cancer subtypes, comprised of estrogen receptor-positive (ER+), progesterone receptor-positive (PR+), human epidermal growth factor receptor-positive (HER2+), and triple negative (ER−, HER2−, and PR−) tumors [16–18]. Recent polymerase chain reaction studies confirmed that FR$\alpha$ is highly expressed in T47D cells [19].

An in vivo theranostic approach combines the potential of both diagnosis and therapy in the same targeting molecule by labeling with either a diagnostic or a suitable therapeutic radionuclide. Theranostic radiotracers provide patients with targeted and personalized treatment options, thereby improving the current clinical treatment options at the same time. In the field of nuclear medicine, $^{177}$Lu-labeled AuNPs conjugated to different peptides have been proposed as a new class of theranostic radiopharmaceuticals [20]. These multifunctional systems contain the chelator DOTA, able to complex both $^{68}$Ga and $^{177}$Lu, which could be useful for the identification of malignant tumors, and monitoring of treatment (SPECT/NIR fluorescence optical imaging), for targeted radiotherapy ($\beta$-particle-energy delivered per unit of targeted mass), and for photothermal therapy (localized heating). Therefore, a multifunctional system of DOTA-dendrimer-AuNP conjugated to bombesin and folate is expected to improve both the recognition of breast cancer cells positive to FR and GRPR and its theranostic properties when labeled with $^{68}$Ga and $^{177}$Lu.

The aim of this work was to synthesize $^{177}$Lu-DOTA-dendrimer-folate-bombesin with gold nanoparticles in the dendritic cavity ($^{177}$Lu-DenAuNP-folate-bombesin) and to evaluate the radiopharmaceutical potential for targeted radiotherapy and the simultaneous detection of FRs and GRPRs overexpressed in T47D breast cancer cells. In order to probe the theranostic potential, the labeling of DenAuNP-folate-bombesin with $^{68}$Ga was also accomplished.

## 2. Materials and Methods

*2.1. Materials.* G4-PAMAM-$(NH_2)_{64}$ dendrimer (10% wt. in methanol, density 0.813 g/mL) [dendrimer] and folic acid were purchased from Sigma-Aldrich Chemical Co. (St. Louis, Missouri, USA). $H_2$N-Lys$^1$Lys$^3$(DOTA)-bombesin (1–14) peptide [bombesin] with a purity of >90% (HPLC) was obtained from piChem Laboratory (Graz, Austria). The bifunctional chelating agent S-2-(4-Isothiocyanatobenzyl)-1,4,7,10-tetraazacyclododecane tetraacetic acid (p-SCN-Bn-DOTA) [DOTA] was obtained from Macrocyclics (Dallas, TX, USA). All other chemicals were also purchased from Sigma-Aldrich Chemical Co. and used without additional purification.

*2.2. Synthesis and Chemical Characterization*

*2.2.1. Conjugation of DOTA to the Dendrimer.* Fifty microliters of dendrimer (0.3 $\mu$mol) in methanol was dried under vacuum and redissolved in 0.5 mL of 0.2 M sodium bicarbonate buffer, pH 9.5. The above solution was then incubated with DOTA (5.38 $\mu$mol; 3.7 mg in 0.5 mL of 0.2 M sodium bicarbonate buffer, pH 9.5) at 37°C during 1 h (DOTA/dendrimer molar ratio of 18/1). The final reaction mixture was washed three times with type I water by ultrafiltration to remove bicarbonate buffer (Ultrafree-PFL Filters, MWCO 10,000, polysulfone membrane, Millipore) and finally lyophilized.

*2.2.2. Activation of Carboxylate Groups of Folic Acid and Bombesin.* Folic acid (2.27 $\mu$mol; 1 mg) and bombesin (0.55 $\mu$mol, 1.1 mg) were dissolved in 200 $\mu$L of dimethylformamide (DMF) and were added to a mixture containing 100 $\mu$L of 0.2 M diisopropylethylamine (DIPEA, to provide a basic medium) (114.83 $\mu$mol; 14.84 mg in 300 $\mu$L of DMF) and 100 $\mu$L of the carboxylate activating agent HATU (O-(7-azabenzotriazol-1-yl)-N,N,N′,N′-tetramethyluronium-hexafluoro phosphate), (15.78 $\mu$mol, 6 mg in 100 $\mu$L of DMF). The reaction mixture was incubated for 15 min at room temperature (20°C).

*2.2.3. Conjugation of Bombesin and Folic Acid to the Amine Groups on the Dendrimer.* The lyophilized DOTA-dendrimer (0.35 $\mu$mol) was dissolved in 100 $\mu$L of DMF and added to the above activated carboxylate folate-bombesin solution. The mixture was incubated during 1.5 h at room temperature. The obtained precipitate was washed with DMF and dried under vacuum. The molar ratio of dendrimer to folate was 1 : 6.5 and 1 : 1.5 for dendrimer to bombesin.

*2.2.4. Synthesis of DenAuNP-Folate-Bombesin.* To an aqueous solution of Den-folate-bombesin (1.4 mg/mL, 0.1 $\mu$mol) 1% $HAuCl_4$ (170 $\mu$L, 5 $\mu$mol) was added under vigorous stirring. After 60 min, 0.56 mL of an ice-cold $NaBH_4$ solution (1 mg/mL, 15 $\mu$mol) was added to the gold dendrimer mixture under stirring. Within a few seconds, the reaction mixture turned deep-red and the stirring process was continued for 2 h to complete the reaction. The final product was purified by ultrafiltration (Ultrafree-PFL Filters, MWCO 10,000, polysulfone membrane, Millipore) and finally lyophilized to obtain DenAuNP-folate-bombesin. For comparative purposes the DenAuNP compound was also prepared under the same procedure.

### 2.3. Chemical Characterization

*2.3.1. IR Spectroscopy.* IR spectra of dendrimer, folate, $Lys^1Lys^3$(DOTA)bombesin (1–14), p-SCN-Bn-DOTA, Den-folate-bombesin, and Den(AuNP)-folate-bombesin, in solid state, were obtained on a Perkin-Elmer System spectrometer (Spectrum 400) (Waltham, MA, USA) with an attenuated total reflection platform (Diamond GLADIATOR, Pike Technologies; Madison, WI, USA), from 500 to 4000 $cm^{-1}$.

*2.3.2. Transmission Electron Microscopy (TEM).* TEM was performed using a JEOL-EMDSC-U10A instrument (JEOL, Japan) operating at 200 kV. The samples of each compound (DenAuNP or DenAuNP-folate-bombesin) were analyzed stained and unstained. The samples were dropped onto a carbon-coated copper grid and allowed to evaporate under vacuum before measurements. Some samples of both compounds were then stained with an aqueous solution of phosphotungstic acid (2% w/w) and dried.

*2.3.3. Dynamic Light Scattering (DLS) and Zeta Potential Measurement.* The DLS and Zeta potential measurement were performed using a Nanotrac Wave (Model MN401, Microtract, FL, USA). The temperature of the cell housing was set to 22.6°C. The data was acquired from DenAuNP and DenAuNP-folate-bombesin samples diluted in MilliQ water ($n = 3$). The hydrodynamic diameter and Zeta potential were obtained for each sample.

*2.3.4. Scanning Electron Microscopy (SEM) and X-Ray Analysis.* The multifunctional DenAuNP-folate-bombesin was visualized by scanning electron microscopy (SEM). The sample was mounted on an aluminum stub using double-sided tape. The coated sample was examined using an electron acceleration voltage of 20–25 keV (JEOL JSM-5900 Low Vacuum, USA). The X-ray analysis was obtained from a selected area of the sample using the above system.

*2.3.5. Fluorescence Spectroscopy.* Emission fluorescence spectra of DenAuNP-folate-bombesin, Den-folate-bombesin, and dendrimer samples in solid state (powder) at 291 K were recorded on a Perkin-Elmer LS-55 low-resolution luminescence spectrometer, from 200 to 900 nm. The best results were obtained using an excitation wavelength ($\lambda_{exc}$) of 222 nm, emission filter of 290 nm, and excitation and emission slits of 5 nm for the three samples.

*2.4. Preparation of $^{68}$Ga-/$^{177}$Lu-DenAuNP-Folate-Bombesin.* Radiolabeling with $^{177}$Lu was carried out by adding $^{177}LuCl_3$ solution (20 $\mu$L, 1.1 GBq, 3 TBq/mg, ITG, Germany) to the DenAuNP or DenAuNP-folate-bombesin conjugate (50 $\mu$g in a solution of 200 $\mu$L of 0.25 M acetate buffer, pH 5.5) and incubating it at 37.5°C for 20 min. For $^{68}$Ga labeling, $^{68}GaCl_3$ was obtained from a $^{68}$Ge/$^{68}$Ga-Generator (ITG, Germany) eluted with 0.5 M HCl to which (1 mL) 50 $\mu$g of DenAuNP-folate-bombesin conjugate was added in a solution of 1 mL of 0.5 M acetate buffer, pH 4.0, incubating it at 90°C for 10 min.

The radiochemical purity was determined using a radio-HPLC size-exclusion system (ProteinPak 300SW, Waters, 1 mL/min, $NaHCO_3$ 0.2 M, pH 9.5). Chromatographic profiles were obtained using two different detectors, the UV-Vis detector and a radiometric detector. The sample first passed through the UV-Vis detector (photodiode array) and after 0.5 min (0.5 mL, 1 mL/min), it passed through the radioactivity detector. The retention times in this system were $t_R = 7.80$ and 8.31 min in the chromatogram and radiochromatogram, respectively. Correspondence in retention times of the peaks of interest in the chromatogram is commonly accepted as a proof of the chemical identity of the radiopharmaceutical. For comparative studies, $^{177}$Lu-folate-bombesin was also prepared as previously reported by Aranda-Lara et al. [21].

### 2.5. In Vitro Studies

*2.5.1. Stability in Human Serum.* To determine the stability of $^{177}$Lu-DenAuNP-folate-bombesin in serum, 200 $\mu$L of radiotracer was diluted at a ratio of 1 : 10 with fresh human serum and incubated at 37°C. Radiochemical stability was determined with a 100 $\mu$L sample taken at 24 h for radio-HPLC size-exclusion analysis (ProteinPak 300SW, Waters, 1 mL/min, PBS).

*2.5.2. Cell Culture.* A T47D human breast cancer cell line (obtained from ATCC, USA) was grown at 37°C with 5% $CO_2$ and 85% humidity in folate-free RPMI-1640 culture medium supplemented with 10% fetal bovine serum and 1% antibiotics (streptomycin and penicillin).

*2.5.3. Cell Uptake Studies.* T47D cancer cells suspended in fresh medium were diluted to $4 \times 10^6$ cells/tube with PBS at pH 7.4 or pH 5.3 (mimicking the acidic conditions within tumors) and incubated with 20 $\mu$L (0.9 MBq) of $^{177}$Lu-DenAuNP-folate-bombesin, $^{177}$Lu-DenAuNP, or $^{177}$Lu-folate-bombesin in triplicate at 37°C for 1 h. The test tubes were centrifuged at 2500 rpm for 5 min and washed with phosphate-buffered saline. Radioactivity in the cell pellet represents both membrane-bound and internalized radiopharmaceutical and was measured in a crystal scintillation well-type detector (Auto In-v-tron 4010, NML, Inc.). The membrane-bound activity was removed with 1 mL of 0.2 M acetic acid/0.5 M NaCl solution added to the cell pellet. The test tubes were centrifuged and the pellet activity, which was considered as internalization, was measured. Blocking studies were carried out in parallel. The cells were preincubated with 100 $\mu$L of folic acid in 0.01 M NaOH (0.5 mM) or 100 $\mu$L of $Lys^3$-bombesin (0.5 mM) for 5 min before addition of the radiopharmaceutical.

### 2.6. In Vivo Uptake

*2.6.1. Animal Model.* In vivo studies in mice were carried out according to the rules and regulations of the Official Mexican Norm 062-ZOO-1999. Athymic mice, 6-7 weeks old and 18–20 g weight, were kept in sterile cages with sterile wood-shaving beds, constant temperature, humidity, noise,

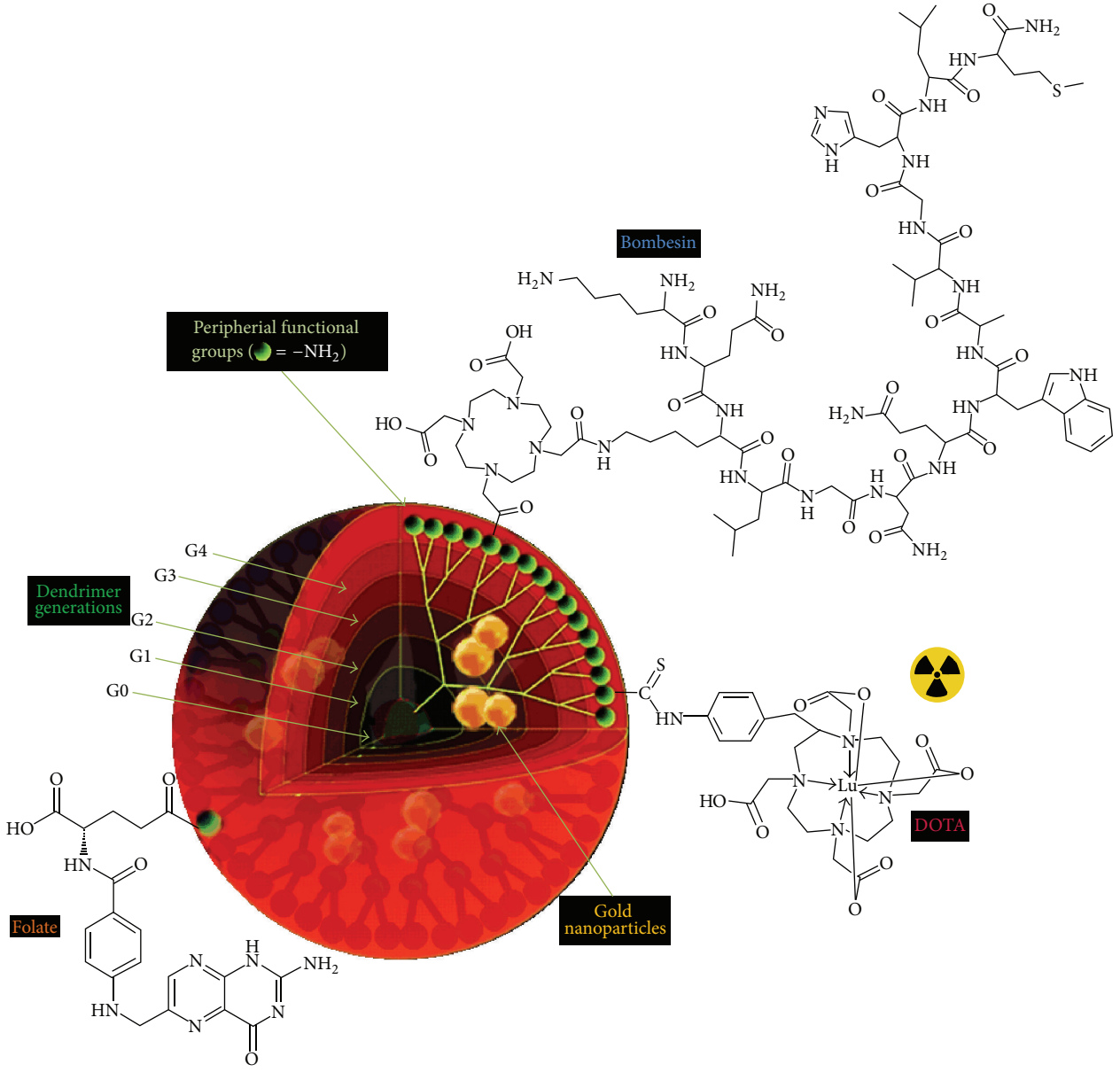


Figure 1: Overall scheme of $^{177}$Lu-DenAuNP-folate-bombesin.

and 12:12 light periods. Athymic mice were maintained on a folate-free diet for 3 weeks before imaging studies.

*2.6.2. Tumor Induction.* Athymic female mice (6-7 weeks old, $n = 4$) were inoculated subcutaneously in the upper back with $2 \times 10^6$ T47D cancer cells suspended in 0.1 mL of phosphate-buffered saline. Injection sites were observed at regular intervals for tumor formation and progression.

*2.6.3. $^{177}$Lu-DenAuNP-Folate-Bombesin Imaging.* To verify the in vivo radionanoconjugate retention in tumors, optical images were acquired at 1 h and 96 h after $^{177}$Lu-DenAuNP-folate-bombesin intratumoral administration (37 MBq) in T47D tumor-bearing mice using a preclinical optical/X-ray imaging system (in vivo X-Treme, Bruker BioSpin Corp., USA). Mice under 2% isoflurane anesthesia were placed in the prone position and whole imaging was performed. Counts in the tumor were quantified at 1 and 48 h after injections.

## 3. Results and Discussion

### 3.1. Synthesis and Chemical Characterization

*Synthesis.* The overall scheme of the theranostic radiopharmaceutical $^{177}$Lu-DenAuNP-folate-bombesin is shown in Figure 1. The DenAuNP-folate-bombesin conjugate was obtained as a black solid with an overall yield of 72%.

*IR Spectroscopy.* The IR spectra of the dendrimer, bombesin, DOTA, folic acid, DenAuNP, Den-folate-bombesin, and

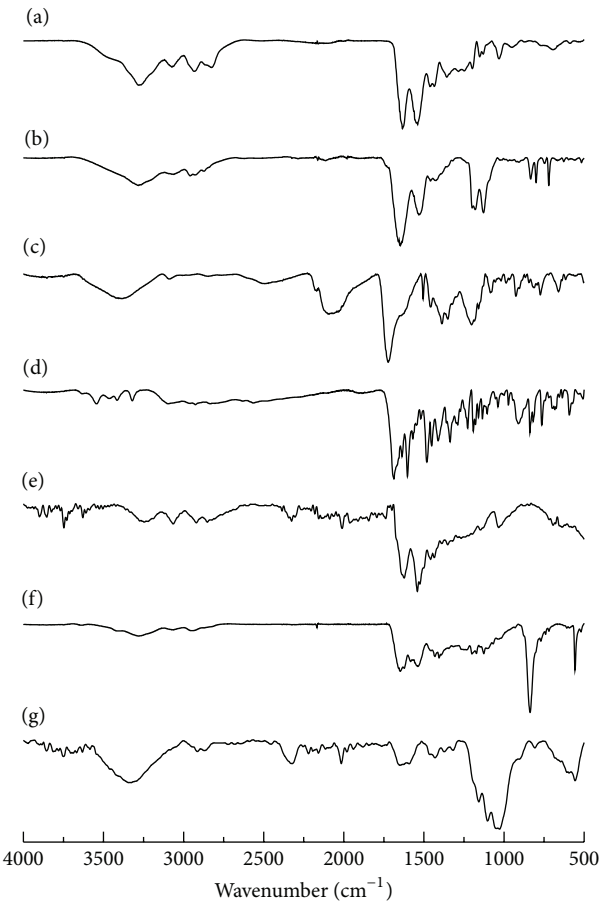


Figure 2: IR-spectrum of (a) dendrimer, (b) bombesin, (c) DOTA, (d) folic acid, (e) DenAuNPs, (f) Den-folate-bombesin, and (g) DenAuNP-folate-bombesin.

DenAuNP-folate-bombesin are presented in Figure 2. The IR-spectrum of Den-folate-bombesin reveals some characteristic bands from the dendrimer, bombesin, DOTA, and folic acid, which change in intensity and positions or disappear because of the conjugation to the dendrimer. In agreement with the IR spectra of bombesin and folic acid described by Aranda-Lara et al. [22], the strong bands in the 1646–1533 cm$^{-1}$ region from the bombesin spectrum (Figure 2(b)) and 1687 cm$^{-1}$ and 1637 cm$^{-1}$ from folic acid (Figure 2(d)) which correspond to amide I and amide II vibrations disappeared or decreased in intensity in the Den-folate-bombesin. A change of symmetry occurs in this supramolecule and bands associated with the formation of new secondary amides increase the absorbance of bands at 839 and 555 cm$^{-1}$, which correspond to a symmetrical C-N-C stretching vibration and to the bending motion of O=C-N group, respectively [23]. In the dendrimer spectrum (Figure 2(a)), three weak well-defined bands at 1152, 1130, and 1032 cm$^{-1}$ are observed. After conjugation (Den-folate-bombesin), the spectrum (Figure 2(f)) revealed two red-shifted bands (7 cm$^{-1}$ and 5 cm$^{-1}$) at 1171 and 1123 cm$^{-1}$, from bombesin: one band at 1033 cm$^{-1}$ from the dendrimer and two semishoulders at 1100 and 1065 cm$^{-1}$, from DOTA (Figure 2(c)) and folic acid (Figure 2(d)). In the DenAuNP spectrum, two bands at 1146 and 1031 cm$^{-1}$, from the dendrimer, are observed and the pattern of the spectrum changed (Figure 2(e)), which indicates the encapsulation of the AuNPs with effect on the molecular symmetry of the dendrimer. Structured new regions between 3900 and 3600 cm$^{-1}$ (centered at 3747 cm$^{-1}$), and between 2250 and 1700 cm$^{-1}$ (centered at 2011 cm$^{-1}$), are observed and seem to correspond to weak hydrogen bonding between the dendrimer amides as the result of the entrapped AuNPs. The change in the spectrum of Den-folate-bombesin after the encapsulation of AuNPs (DenAuNP-folate-bombesin) (Figure 2(g)) suggests a new molecule with particular physicochemical properties. The weak bands between 1200 and 900 cm$^{-1}$ observed in Den-folate-bombesin spectrum are the most strong in that of DenAuNP-folate-bombesin. The bands at 1157 and 1029 cm$^{-1}$ are from the dendrimer and those at 1102 and 1051 cm$^{-1}$ (14 cm$^{-1}$ red-shifted) are from the molecules conjugated to the dendrimer (Figure 2(g)). Their increase in absorbance seems to be the result of the encapsulation of AuNPs in the dendritic cavity. The bands observed between 1200 and 1000 cm$^{-1}$ correspond to C-N stretching vibrations from primary amides, secondary amides, and tertiary aliphatic amines [23]. In particular, CN vibrations from tertiary aliphatic amines are located between 1040 and 1020 cm$^{-1}$ [23].

In the DenAuNP-folate-bombesin spectrum, two new structured regions with two maximum bands at 3753 and 2015 cm$^{-1}$ slightly blue shifted with respect to those of the DenAuNP are observed, which demonstrates that the entrapped AuNPs favored weak interactions in the dendrimer cavity.

IR suggests that AuNPs are entrapped in the dendritic cavity in Den-AuNPs and in Den-AuNP-folate-bombesin, but in the former the bands of the dendrimer are not strong. In contrast, the conjugation of bombesin, folic acid, and DOTA to the dendrimer induces a particular structural arrangement which allows the encapsulation of the AuNPs in the dendritic cavity and affords a larger stability and an adequate symmetry to the supramolecule, which is revealed in the particular feature of the spectrum and the very strong bands associated with the -C-N- groups.

*Transmission Electron Microscopy*. TEM images of DenAuNP-folate-bombesin (Figure 3(a)) show single units of the compounds as grayish round objects with a mean diameter of 5.6± 0.4 nm, which is slightly greater than that of DenAuNP (4.53± 1.33 nm, Figure 3(b)) because of the conjugation with folate and bombesin. The increase in the hydrodynamic diameter of DenAuNP-folate-bombesin by the conjugation effect was observed by TEM as a halo around the compound due to the poor interaction of the electron beam with the folate and bombesin molecules (low electron density), in contrast to the strong scattering of the electron beam when it interacted with the metallic nanoparticles [24]. Each compound shows small black dots that correspond to the gold nanoparticles with approximate average diameter of 2.5±0.4 nm. According

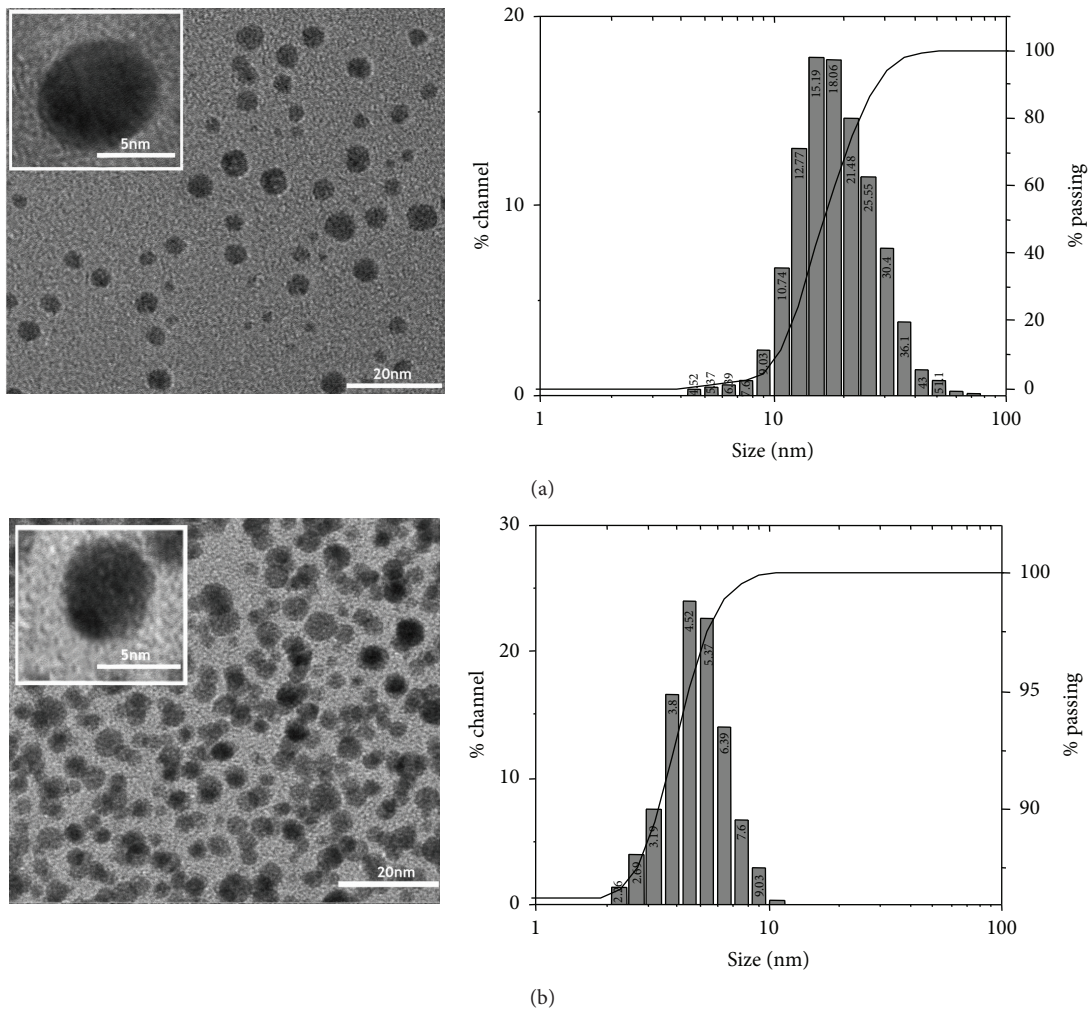


Figure 3: TEM image and size distribution (DLS) of (a) DenAuNP-folate-bombesin and (b) DenAuNP.

to the previous studies, the black dots indicate that gold nanoparticles are in the dendritic cavity [25].

*Particle Size and Zeta Potential.* The hydrodynamic diameter of DenAuNPs and DenAuNP-folate-bombesin by DLS was 5.00 ± 1.47 nm and 18.60 ± 8.00 nm, respectively (Figure 3). The $Z$ potential of the DenAuNP-folate-bombesin was 86.3 ± 3.8 mV, versus 28.6 ± 2.7 mV for the DenAuNPs, indicating that the folate and bombesin conjugation confers a high colloidal stability to the multifunctional system.

*Scanning Electron Microscopy*. The SEM image (Figure 4(a)) showed that the DenAuNP-folate-bombesin conjugate has a granular and homogeneous structure. The qualitative elemental content determined by X-ray analysis for DenAuNP-folate-bombesin (Figure 4(b)) shows the presence of Au and S as well as C, N, and O.

*UV-Vis*. The Den-folate-bombesin spectrum showed bands associated with DOTA (shoulder at 258 nm), bombesin (278 nm), and folate (284 nm and a shoulder at 340 nm) (Figure 5(a)), which were masked in the presence of the entrapped AuNPs (Figure 5(b)). The DenAuNP-folate-bombesin spectrum exhibited a surface plasmon resonance as a shoulder at approximately 510 nm (Figure 5(b)). The plasmon band is associated with the average contribution of the entire AuNP population, but only the AuNPs with diameters larger than 2.5 nm significantly contribute to the plasmon band absorption at 510 nm [25, 26]. Several groups have reported the presence of intradendrimer encapsulated nanoparticles, in which the nanoparticle resides within the interior void space of the dendrimer, as well as interdendrimer-stabilized nanoparticles, in which the nanoparticle surface is stabilized by multiple dendrimers through their terminal amine groups. Intradendrimer nanoparticles are usually smaller than 4.5 nm; in contrast, interdendrimer particles are always larger than 5 nm [26]. In this research, the encapsulation of 2.1–2.9 nm diameter nanoparticles within single dendrimers observed in TEM images suggests that formation of gold interdendrimer particles did not occur, possibly due to the

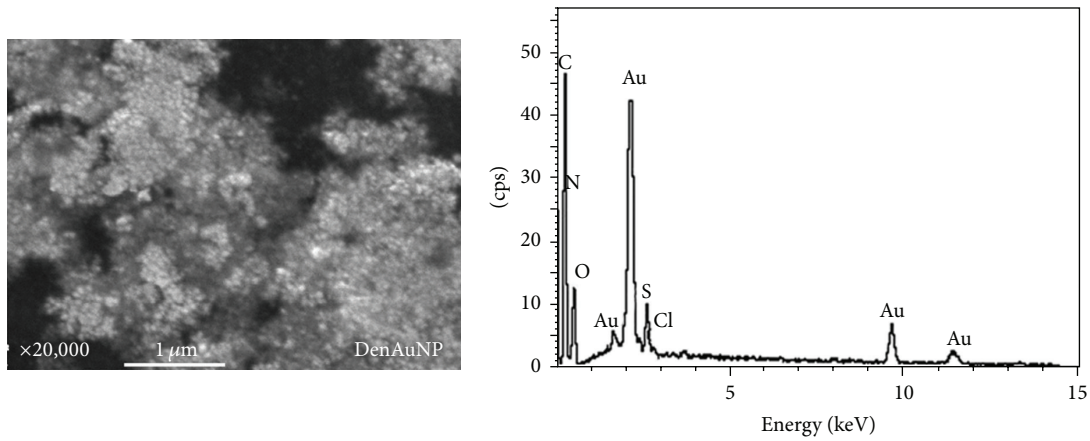


Figure 4: SEM image (a) and X-ray analysis (b) for DenAuNP-folate-bombesin.

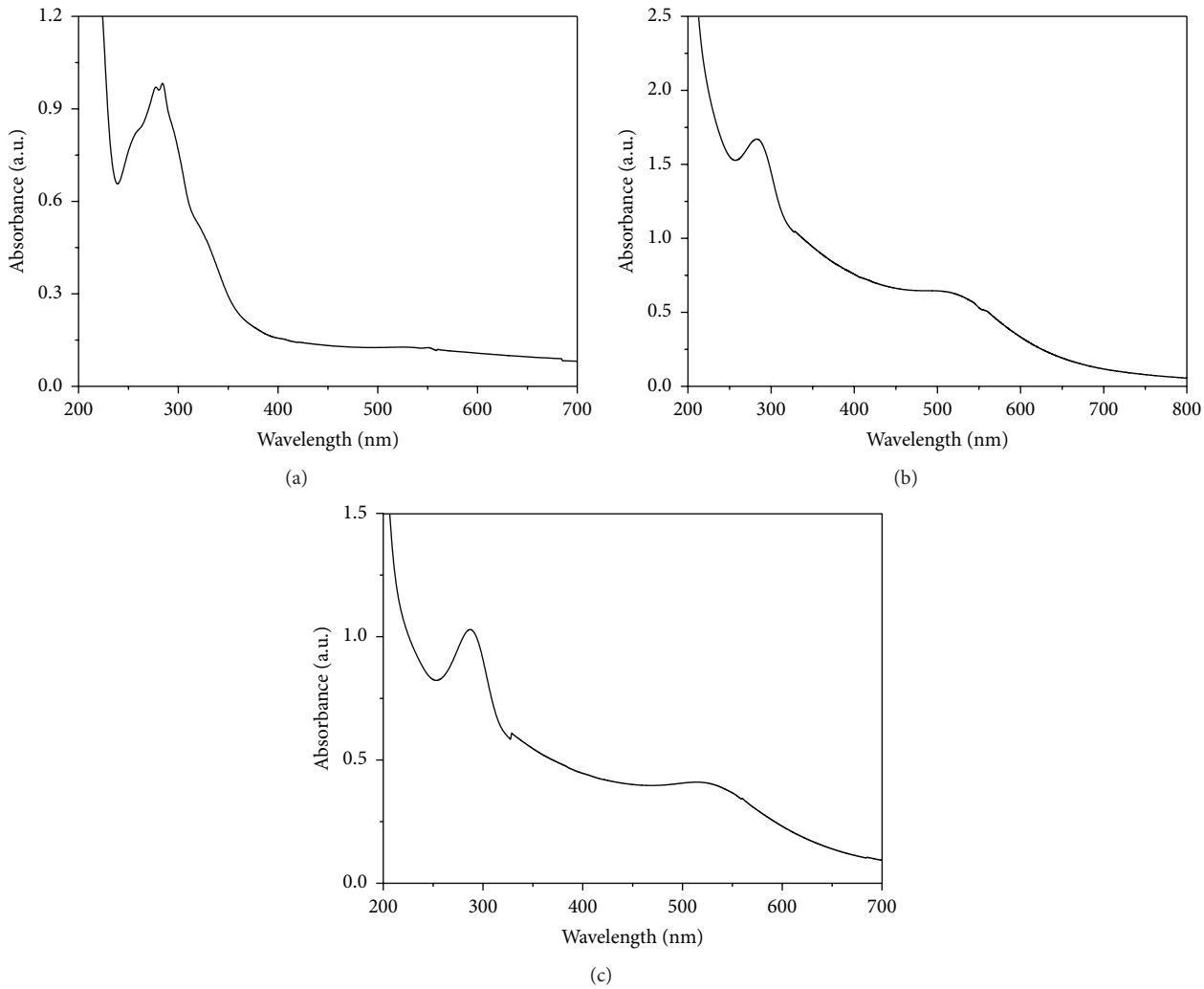


Figure 5: UV-Vis spectra in aqueous media of (a) Den-folate-bombesin, (b) DenAuNP-folate-bombesin, and (c) DenAuNP.

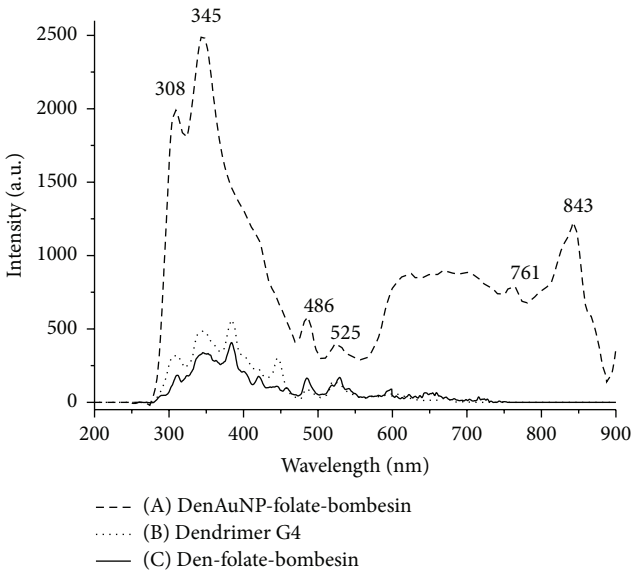


Figure 6: Emission fluorescence spectra in powder at 291 K of (A) DenAuNP-folate-bombesin, (B) Den-folate-bombesin ($\lambda_{emi}$ = 311, 347, 383, 421, 444, 485, and 529 nm), and dendrimer ($\lambda_{emi}$ = 308, 345, 384, 419, 445, 484, and 520 nm). The three spectra were measured at $\lambda_{exc}$ = 222 nm, slit$_{exc}$ = 5.0 nm, slit$_{emi}$ = 5.0 nm, and filter = 290 nm.

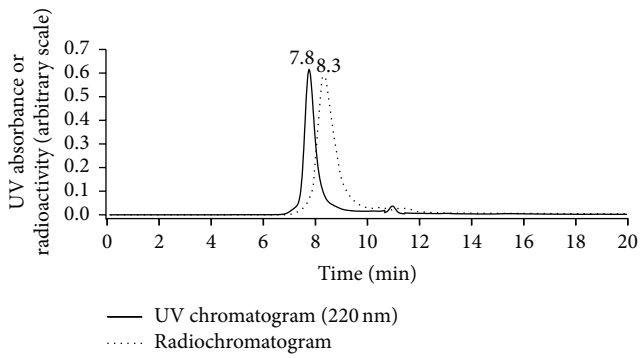


Figure 7: Size-exclusion HPLC chromatogram (220 nm; continuous line) and HPLC radiochromatogram (dotted line) of the $^{177}$Lu-DenAuNP-folate-bombesin theranostic radiopharmaceutical (flow rate 1 mL/min). $^{68}$Ga-DenAuNP-folate-bombesin showed the same retention time (7.8 ± 0.2 min).

steric effect of bombesin, folate, and DOTA on the dendrimer surface. The band at 290 nm is reproducibly observed during the syntheses of AuNPs through the use of dendrimers as templates [27]. This band and the plasmon band absorption are also observed in the DenAuNPs spectrum (Figure 5(c)).

The surface plasmon resonance observed at 510 nm opens the possibility for further studies related to plasmonic photothermal therapy [28]. Several trials have demonstrated a significant improvement in the clinical outcome when radiotherapy was conducted under hyperthermic conditions in patients [29]. Hyperthermia increases the efficacy of radiotherapy by improving tumor oxygenation and interfering with the DNA repair mechanisms. By exposing $^{177}$Lu-DenAuNP-folate-bombesin to laser irradiation, it could be possible to heat a localized area in the tumor without any harmful heating of the surrounding healthy tissues.

*Fluorescence Spectroscopy*. Figure 6 shows the selected fluorescence emission spectra of the dendrimer, Den-folate-bombesin, and Den-AuNP-folate-bombesin from the luminescence studies. Two important aspects are observed, the enhanced luminescence of the DenAuNP-folate-bombesin (Figure 6(A)) with respect to the dendrimer and Den-folate-bombesin, and the presence of new peaks at 761 and 843 nm. The high luminescence intensity is caused by the encapsulated small AuNPs that induce the stabilization of the molecule and the NIR emissions. This fact pointed to the presence of NIR-emitting gold nanoclusters (NCs), possibly in the form of $(Au^0)_{50}$-dendrimer-G4. Recent developments in the NC field have demonstrated that metal NCs are excellent luminescent materials [3, 30]. The luminescent properties of the DenAuNP-folate-bombesin conjugate are relevant because it could be used in animal imaging. Recently, Wu et al. investigated tumor targeting of NIR-emitting BSA-stabilized AuNCs, and the NIR fluorescence significantly improved tissue penetration depth up to few millimeters [31].

*Radiolabeling*. The size-exclusion HPLC chromatogram and radiochromatogram of the purified multifunctional system (Figure 7) show that both $^{68}$Ga- or $^{177}$Lu-DenAuNP-folate-bombesin were obtained with a radiochemical purity of 97 ± 2%, without postlabeling purification ($n$ = 20). After incubation of the $^{177}$Lu-DenAuNP-folate-bombesin radiopharmaceutical in human serum (24 h at 37°C), the radio-HPLC chromatogram showed a radiochemical purity of >90%, which demonstrates its high stability in serum.

*3.2. T47D Cancer Cell Studies*. Preliminary cell studies showed an important uptake of $^{177}$Lu-DenAuNP-folate-bombesin in T47D cancer cells, which was significantly ($t$-student, $p < 0.05$) inhibited by preincubation with cold Lys$^3$-bombesin peptide or folic acid alone, indicating that the multifunctional system has specific recognition for GRPRs and FRs (Figure 8). The T47D cell uptake of $^{177}$Lu-DenAuNP was 9.84 ± 1.14%, mainly attributed to a passive uptake mechanism [24], and significantly ($t$-student, $p < 0.05$) lower than that of $^{177}$Lu-DenAuNP-folate-bombesin (41.15 ± 2.72%).

At pH 7.4, the preincubation with cold Lys$^3$-bombesin showed greater blocking effect on the multifunctional system (62.14% less uptake) compared with that of the cold folic acid (36.53% less uptake) (Figure 8). This difference in blocking effect is consistent with the GRP and folate receptors' expression levels in T47D breast cancer cells [21, 22], which suggest that the specific targeting of the $^{177}$Lu-DenAuNP-folate-bombesin in T47D is mainly dominated by the specific recognition of the bombesin moiety through GRP receptors. It is important to mention that, at pH = 5.3 and in the presence of cold bombesin or cold folic acid in blocking studies, the

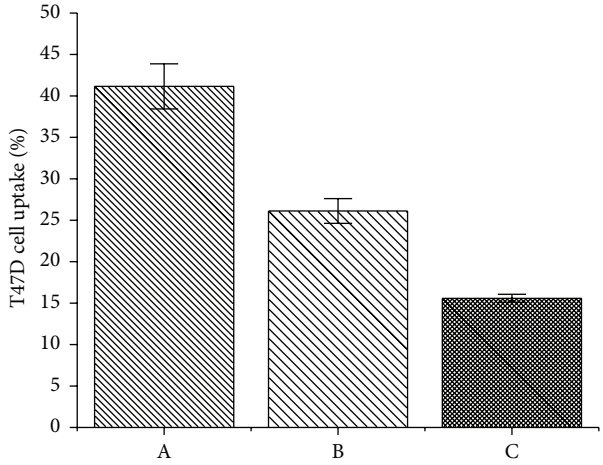


FIGURE 8: In vitro uptake of $^{177}$Lu-DenAuNP-folate-bombesin in T47D breast cancer cells at 1 h. (A) Unblocked, (B) blocked with folic acid, and (C) blocked with Lys$^3$-bombesin.

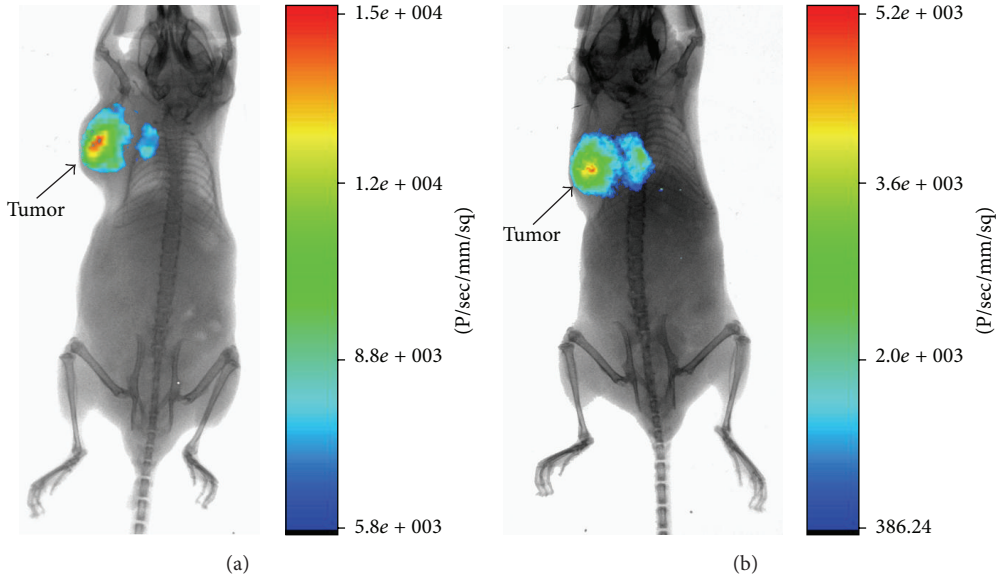


FIGURE 9: Optical imaging of $^{177}$Lu-DenAuNP-folate-bombesin at 1 h and 96 h after intratumoral administration.

observed effect is an increase in the $^{177}$Lu-DenAuNP-folate-bombesin cell uptake (77.6 ± 9.5%) possibly related to the dendrimer cellular adsorption [32].

The in vitro T47D cell uptake was higher for $^{177}$Lu-DenAuNP-folate-bombesin (41.15 ± 2.72%) than that reported for the $^{177}$Lu-folate-bombesin conjugate (33.27 ± 2.52%) [22]. This effect could be associated with the multivalent ligand-receptor binding of the $^{177}$Lu-DenAuNP-folate-bombesin, since the peptide-nanoparticle conjugate provides a surface for simultaneous interactions with the cell surface, giving rise to multivalent effects (defined as an affinity enhancement) [24], as well as to the contribution of dendrimer passive uptake [24]. Nevertheless, further studies related to cell internalization and affinity must be carried out.

Preliminary in vivo imaging studies demonstrated that $^{177}$Lu-DenAuNP-folate-bombesin remained in the T47D tumor up to 96 h after intratumoral radiopharmaceutical administration, since in all mice the tumor intensity in the optical imaging correlated with the radionuclide decay (e.g., at 1 h = 11354 photons/s/mm$^2$; at 96 h = 6830 photons/s/mm$^2$) with only 9 ± 5% of biological elimination (Figure 9).

Considering that one Becquerel (Bq) of Lu-177 produces 841558 disintegrations until total decay (total disintegrations = $\int_0^t A(t)dt$) with a maximum $\beta^-$-particle energy of 0.498 MeV, it is expected that, with the high $^{177}$Lu-DenAuNP-folate-bombesin retention observed in tumors, the total radiation absorbed dose to the malignant tissue could easily reach 2 Gy per MBq [33]. However, further preclinical studies must

be carried out in order to evaluate the toxicity, biokinetics, and dosimetry of this radiopharmaceutical.

An important benefit of receptor-specific radiopharmaceuticals is their potential for use in targeted radiotherapy. Multiple peptides, specific to target receptors that are overexpressed in breast cancer cells, appended to one nanoparticle and radiolabeled with an imaging and $\beta^-$ particle-emitting radionuclide ($^{177}$Lu), act as a multifunctional system that could be useful in identifying malignant tumors and metastatic sites (by single photon emission computed tomography imaging, "SPECT"), for targeted radiotherapy (high $\beta$-particle-energy delivered per unit of targeted mass), and for thermal therapy (localized heating after laser irradiation). However, for therapeutic purposes, NPs should be administered by intratumoral injection or into a selective artery to avoid high uptake by organs of the reticuloendothelial system due to the colloidal nature of NPs [33]. Injection into a breast tumor would allow high uptake into a tumor, possible micrometastases, or individual cancer cells. Therefore, $^{177}$Lu-DenAuNP-folate-bombesin has potential application in medical diagnosis and therapeutic treatments due to its unique combination of radioactive, optical, and thermoablative properties. This study demonstrated that the nanosystem exhibited chemical and physical properties that are suitable for plasmonic photothermal therapy and targeted radiotherapy in the treatment of breast cancer.

## 4. Conclusions

Elemental analysis and spectroscopy techniques showed that folic acid, bombesin, and DOTA molecules were successfully conjugated to one molecule of the PAMAM dendrimer. Chromatographic studies showed that the $^{68}$Ga- and $^{177}$Lu-DenAuNP-folate-bombesin conjugate were obtained with high radiochemical purity (>95%). Preliminary binding studies in T47D breast cancer cells indicated a specific cell uptake and high retention in T47D-induced tumors in mice.

Luminescence results show that AuNPs in the conjugate increase the fluorescence intensity, resulting in a multifunctional system that may be useful as an optical and nuclear imaging agent for breast tumors overexpressing GRPRs and FRs, as well as for targeted radiotherapy.

## Competing Interests

The authors declare that there is no conflict of interests regarding the publication of this paper.

## Acknowledgments

This study was supported by the Mexican National Council of Science and Technology (CONACYT-SEP-CB-2014-01-242443) and the International Atomic Energy Agency (Grant 18358). This research was carried out as part of the activities of the "Laboratorio Nacional de Investigación y Desarrollo de Radiofármacos, CONACyT."

## References

[1] D. Astruc, E. Boisselier, and C. Ornelas, "Dendrimers designed for functions: from physical, photophysical, and supramolecular properties to applications in sensing, catalysis, molecular electronics, photonics, and nanomedicine," *Chemical Reviews*, vol. 110, no. 4, pp. 1857–1959, 2010.

[2] P. Szymański, M. Markowicz, and E. Mikiciuk-Olasik, "Nanotechnology in pharmaceutical and biomedical applications. Dendrimers," *Nano*, vol. 6, no. 6, pp. 509–539, 2011.

[3] C. Zhou, S. Yang, J. Liu, M. Yu, and J. Zheng, "Luminescent gold nanoparticles: a new class of nanoprobes for biomedical imaging," *Experimental Biology and Medicine*, vol. 238, no. 11, pp. 1199–1209, 2013.

[4] C. Zhou, J. Yu, Y. Qin, and J. Zheng, "Grain size effects in polycrystalline gold nanoparticles," *Nanoscale*, vol. 4, no. 14, pp. 4228–4233, 2012.

[5] V. Sancho, A. Di Florio, T. W. Moody, and R. T. Jensen, "Bombesin receptor-mediated imaging and cytotoxicity: review and current status," *Current Drug Delivery*, vol. 8, no. 1, pp. 79–134, 2011.

[6] S. U. Dalm, J. W. M. Martens, A. M. Sieuwerts et al., "In vitro and in vivo application of radiolabeled gastrin-releasing peptide receptor ligands in breast cancer," *Journal of Nuclear Medicine*, vol. 56, no. 5, pp. 752–757, 2015.

[7] C. L. Santos-Cuevas, G. Ferro-Flores, C. A. de Murphy, and P. A. Pichardo-Romero, "Targeted imaging of gastrin-releasing peptide receptors with 99mTc-EDDA/HYNIC-[Lys3]-bombesin: biokinetics and dosimetry in women," *Nuclear Medicine Communications*, vol. 29, no. 8, pp. 741–747, 2008.

[8] F. Scopinaro, A. D. Varvarigou, W. Ussof et al., "Technetium labeled bombesin-like peptide: preliminary report on breast cancer uptake in patients," *Cancer Biotherapy and Radiopharmaceuticals*, vol. 17, no. 3, pp. 327–335, 2002.

[9] F. Shariati, K. Aryana, A. Fattahi et al., "Diagnostic value of 99mTc-bombesin scintigraphy for differentiation of malignant from benign breast lesions," *Nuclear Medicine Communications*, vol. 35, no. 6, pp. 620–625, 2014.

[10] C. Van de Wiele, P. Phonteyne, P. Pauwels et al., "Gastrin-releasing peptide receptor imaging in human breast carcinoma versus immunohistochemistry," *Journal of Nuclear Medicine*, vol. 49, no. 2, pp. 260–264, 2008.

[11] S. Ait-Mohand, P. Fournier, V. Dumulon-Perreault et al., "Evaluation of 64Cu-labeled bifunctional Chelate-Bombesin conjugates," *Bioconjugate Chemistry*, vol. 22, no. 8, pp. 1729–1735, 2011.

[12] J. J. Parry, R. Andrews, and B. E. Rogers, "MicroPET imaging of breast cancer using radiolabeled bombesin analogs targeting the gastrin-releasing peptide receptor," *Breast Cancer Research and Treatment*, vol. 101, no. 2, pp. 175–183, 2007.

[13] A. F. Prasanphanich, L. Retzloff, S. R. Lane et al., "In vitro and in vivo analysis of [$^{64}$Cu-$NO_2$A-8-Aoc-BBN(7–14)$NH_2$]: a site-directed radiopharmaceutical for positron-emission tomography imaging of T-47D human breast cancer tumors," *Nuclear Medicine and Biology*, vol. 36, no. 2, pp. 171–181, 2009.

[14] L. E. Kelemen, "The role of folate receptor $\alpha$ in cancer development, progression and treatment: cause, consequence or innocent bystander?" *International Journal of Cancer*, vol. 119, no. 2, pp. 243–250, 2006.

[15] L. Teng, J. Xie, L. Teng, and R. J. Lee, "Clinical translation of folate receptor-targeted therapeutics," *Expert Opinion on Drug Delivery*, vol. 9, no. 8, pp. 901–908, 2012.

[16] B. M. Necela, J. A. Crozier, C. A. Andorfer et al., "Folate receptor-$\alpha$ (FOLR1) expression and function in triple negative tumors," *PLoS ONE*, vol. 10, no. 3, Article ID e0122209, 2015.

[17] D. J. O'Shannessy, E. B. Somers, J. Maltzman, R. Smale, and Y.-S. Fu, "Folate receptor alpha (FRA) expression in breast cancer: identification of a new molecular subtype and association with triple negative disease," *SpringerPlus*, vol. 1, no. 1, pp. 1–9, 2012.

[18] Z. Zhang, J. Wang, D. E. Tacha et al., "Folate receptor $\alpha$ associated with triple-negative breast cancer and poor prognosis," *Archives of Pathology and Laboratory Medicine*, vol. 138, no. 7, pp. 890–895, 2014.

[19] J. Renukuntla, S. Shah, S. Boddu et al., "Functional characterization and expression of folate receptor-$\alpha$ in T47D human breast cancer cells," *Drug Development and Therapeutics*, vol. 6, no. 2, pp. 52–61, 2015.

[20] G. Ferro-Flores, B. E. Ocampo-García, C. L. Santos-Cuevas, F. de María Ramírez, E. P. Azorín-Vega, and L. Meléndez-Alafort, "Theranostic radiopharmaceuticals based on gold nanoparticles labeled with $^{177}$Lu and conjugated to peptides," *Current Radiopharmaceuticals*, vol. 8, no. 2, pp. 150–159, 2015.

[21] L. Aranda-Lara, G. Ferro-Flores, F. D. M. Ramírez et al., "Improved radiopharmaceutical based on 99mTc-Bombesin–folate for breast tumour imaging," *Nuclear Medicine Communications*, vol. 37, no. 4, pp. 377–386, 2016.

[22] L. Aranda-Lara, G. Ferro-Flores, E. Azorín-Vega et al., "Synthesis and evaluation of Lys1($\alpha$,$\gamma$-Folate)Lys3(177Lu-DOTA)-Bombesin(1-14) as a potential theranostic radiopharmaceutical for breast cancer," *Applied Radiation and Isotopes*, vol. 107, pp. 214–219, 2016.

[23] G. Socrates, *Infrared and Raman Characteristic Group Frequencies: Tables and Charts*, John Wiley & Sons, New York, NY, USA, 2004.

[24] E. Orocio-Rodríguez, G. Ferro-Flores, C. L. Santos-Cuevas et al., "Two novel nanosized radiolabeled analogues of somatostatin for neuroendocrine tumor imaging," *Journal of Nanoscience and Nanotechnology*, vol. 15, no. 6, pp. 4159–4169, 2015.

[25] J. C. Garcia-Martinez and R. M. Crooks, "Extraction of Au nanoparticles having narrow size distributions from within dendrimer templates," *Journal of the American Chemical Society*, vol. 126, no. 49, pp. 16170–16178, 2004.

[26] X. Shi, S. Wang, H. Sun, and J. R. Baker Jr., "Improved biocompatibility of surface functionalized dendrimer-entrapped gold nanoparticles," *Soft Matter*, vol. 3, no. 1, pp. 71–74, 2007.

[27] Y.-G. Kim, S.-K. Oh, and R. M. Crooks, "Preparation and characterization of 1-2 nm dendrimer-encapsulated gold nanoparticles having very narrow size distributions," *Chemistry of Materials*, vol. 16, no. 1, pp. 167–172, 2004.

[28] H. Mendoza-Nava, G. Ferro-Flores, B. Ocampo-García et al., "Laser heating of gold nanospheres functionalized with octreotide: in vitro effect on hela cell viability," *Photomedicine and Laser Surgery*, vol. 31, no. 1, pp. 17–22, 2013.

[29] R. A. M. Canters, M. M. Paulides, M. F. Franckena, J. van der Zee, and G. C. van Rhoon, "Implementation of treatment planning in the routine clinical procedure of regional hyperthermia treatment of cervical cancer: an overview and the Rotterdam experience," *International Journal of Hyperthermia*, vol. 28, no. 6, pp. 570–581, 2012.

[30] N. Goswami, Q. Yao, Z. Luo, J. Li, T. Chen, and J. Xie, "Luminescent metal nanoclusters with aggregation-induced emission," *The Journal of Physical Chemistry Letters*, vol. 7, no. 6, pp. 962–975, 2016.

[31] X. Wu, X. He, K. Wang, C. Xie, B. Zhou, and Z. Qing, "Ultrasmall near-infrared gold nanoclusters for tumor fluorescence imaging in vivo," *Nanoscale*, vol. 2, no. 10, pp. 2244–2249, 2010.

[32] S. Parimi, T. J. Barnes, D. F. Callen, and C. A. Prestidge, "Mechanistic insight into cell growth, internalization, and cytotoxicity of PAMAM dendrimers," *Biomacromolecules*, vol. 11, no. 2, pp. 382–389, 2010.

[33] M. Luna-Gutiérrez, G. Ferro-Flores, B. Ocampo-García et al., "$^{177}$Lu-labeled monomeric, dimeric and multimeric RGD peptides for the therapy of tumors expressing $\alpha(\nu)\beta(3)$ integrins," *Journal of Labelled Compounds and Radiopharmaceuticals*, vol. 55, no. 4, pp. 140–148, 2012.